Targeting cysteine-rich angiogenic inducer-61 by antibody immunotherapy suppresses growth and migration of non-small cell lung cancer

XINPENG LI[1,2], NAXIN YUAN[2], LINGDAN LIN[3], LIXIA YIN[2] and YIQING QU[1]

[1]Department of Respiration, Qilu Hospital of Shandong University, Jinan, Shandong 250012; Departments of [2]Respiration and [3]Cardiology, Dezhou People's Hospital, Dezhou, Shandong 253014, P.R. China

Received April 1, 2016; Accepted March 17, 2017

DOI: 10.3892/etm.2018.6274

Abstract. Non-small cell lung cancer (NSCLC) is the most frequent type of human lung cancer; lung cancer is responsible for the highest rates of cancer-associated mortality in the world. Cysteine-rich angiogenic inducer-61 (CYR-61) has been identified as a tumorigenesis-, development- and metastasis-related gene, and is reported to enhance proliferation, migration and invasion through hepatocyte growth factor (HGF)-induced scattering and the metastasis-inducing HGF/Met signaling pathway in tumor cells and xenograft models. CYR-61 is a protein that promotes human lung cancer cell metastasis and is closely related to the patient's prognosis in NSCLC. The purpose of the present study was to investigate whether CYR-61 may serve as a dual potential target for gene therapy of human NSCLC. In the present study, an antibody targeted against CYR-61 (anti-CYR-61) was constructed and the therapeutic effects and underlying mechanism of this antibody in NSCLC cells and mice with NSCLC was investigated. It was observed that NSCLC cell viability, migration and invasion were inhibited while cell apoptosis was induced by the neutralization of CYR-61 protein by anti-CYR-61. Western blotting demonstrated that extracellular signal-regulated kinase (ERK) and protein kinase B (AKT) expression levels in NSCLC cells were decreased following treatment with anti-CYR-61. In addition, it was observed that inhibition of NSCLC cell viability was achieved by the suppression of the epithelial-mesenchymal transition signaling pathway. ERK and AKT phosphorylation levels were downregulated in NSCLC cells and tumors following anti-CYR-61 treatment. Analysis of a murine model indicated that tumor growth was inhibited and tumor metastasis was significantly suppressed ($P<0.01$) following anti-CYR-61 treatment for CYR-61. In conclusion, CYR-61 may serve as a potential target for gene therapy for the treatment of human NSCLC.

Correspondence to: Professor Yiqing Qu, Department of Respiration, Qilu Hospital of Shandong University, 107 Shandong Jinan West Road, Jinan, Shandong 250012, P.R. China
E-mail: qingyiqu151@163.com

Key words: cysteine-rich angiogenic inducer-61, anti-cysteine-rich angiogenic inducer-61, apoptosis, migration, extracellular signal-regulated kinases, protein kinase B, non-small cell lung cancer

Introduction

Lung cancer is a respiratory disease that is responsible for the highest rates of cancer-associated mortality and air contamination worldwide (1). Small cell lung cancer (SCLC) and non-small cell lung cancer (NSCLC) are two main types of human lung cancer that are characterized by tumor morphology (2), and they account for ~95% of all lung cancer (3). NSCLC which has the highest incidence among all kinds of cancer originates from non-small cells in the lungs (4). NSCLC, which is also the most frequent type of lung cancer, can be divided into squamous cell carcinoma, large cell carcinoma and adenocarcinoma determined by tumor cell genetics. According to the clinical statistics investigations of lung cancer cases >80% of newly diagnosed NSCLC patients were in middle or severe stage (5-7).

Though increasing research has endeavored to improve the efficacy of treatment for patients with NSCLC, the survival rate remained poor, with <15% survival observed in the 5 years after clinical treatment (6,8,9). In addition, the majority of newly diagnosed patients with NSCLC are in the advanced stage. Previous research has reported that migration and invasion in NSCLC are predominantly responsible for the poor survival rate during treatment and recurrence for patients with NSCLC (10,11). As a result, the exploration for effective agents for the inhibition of migration and invasion has become critically important for the treatment of cancer patients (12,13). The present study investigated H358 NSCLC cell migration and invasion. Furthermore, the inhibitory effects of anti-cysteine-rich angiogenic inducer-61 (CYR-61) on H358 NSCLC cell migration and invasion were analyzed *in vitro* and *in vivo*.

CYR-61 is a member of the CYR-61/connective tissue growth factor/nephroblastoma overexpressed (CCN) protein family (14). Previous studies have demonstrated that CYR-61 promotes human lung cancer cell migration and metastasis and it is closely related to patient prognosis in NSCLC (15,16). In addition, CYR-61 is involved in tumor cell mitogenesis, cellular adhesion, migration, differentiation, wound healing, angiogenesis and

survival (17). Previous reports have demonstrated the important roles of CYR-61 in cancer development and metastasis, indicating that CYR-61 may be an important target for gene therapy and tumor suppression (16, 17). In addition, CYR61 has been demonstrated to induce angiogenesis by supplying oxygen for tumor cells during proliferation (18).

Many studies have focused on the functions of the CCN protein family in cancer biology (17,19). A study by Barnett *et al* (7) reported that CYR-61 demonstrated potential as an oncogene or a tumor suppressor, depending on tumor cell type. Clinically, expression of CYR-61 has been associated with the prognosis of breast cancer and prostate cancer (20). However, few studies have investigated the function of CYR-61 in NSCLC. Therefore, the present study investigated the expression of CYR-61 in NSCLC cells and tumors. Results indicated that CYR-61 was expressed at higher levels in NSCLC cells, when compared with normal lung cells of MRC-5. Furthermore, an antibody against CYR-61 (anti-CYR-61) was constructed and its therapeutic effects in mice with NSCLC were investigated.

Recently, numerous studies have indicated that mechanistic target of rapamycin (mTOR) may regulate tumor cell growth, migration and cancer metastasis (21,22). Epithelial-mesenchymal transition (EMT) has an essential role in tumor growth, migration and cancer metastasis. In addition, the EMT process reduces tumor cell adhesion and results in tumor cells gaining migratory and invasive properties through cell-cell connections (23). Previous research has indicated that CYR-61 is associated with NSCLC migration and cancer metastasis (17). However, little is known about the signaling mechanisms regulating mTOR, CYR-61 and EMT in NSCLC. Therefore, the present study examined the association between CYR-61 and EMT in NSCLC cells. EMT biomarker expression levels of vimentin, fibronectin, α-smooth muscle actin (SMA) and N-cadherin were analyzed. Mitogen-activated protein kinase (MAPK) and phosphoinositide 3-kinase (PI3K)/protein kinase B (AKT)/mTOR signaling pathways in EMT were also investigated *in vitro* and *in vivo* in NSCLC cells and tissues, respectively.

The aim of the present study was to determine the effects of anti-CYR-61 on CYR-61-associated invasion and metastasis in NSCLC through MAPK/EMT signaling pathways. It was concluded that CYR-61 may be considered as a potential prognostic biomarker for NSCLC, and anti-CYR-61 may provide a potential minimally invasive therapy for NSCLC.

Materials and methods

Ethics statement. The present study was carried out in strict accordance with the approval and recommendations from the Ethics Committee of the Care and Use of Laboratory Animals of Qilu Hospital of Shandong University (Jinan, China). All surgery and euthanasia were performed under sodium pentobarbital anesthesia, and all efforts were made to minimize suffering.

Cell culture. The H358 NSCLC cell line and MRC-5 normal lung cell line were purchased from American Type Culture Collection (Manassas, VA, USA). The cell lines were cultured in RPMI-1640 medium (Gibco; Thermo Fisher Scientific, Inc., Waltham, MA, USA) supplemented with 10% fetal bovine serum (Sigma-Aldrich; Merck KGaA, Darmstadt, Germany) at 37˚C, 5% CO_2 and 100% humidity.

Construction of full-length anti-CYR-61 antibody. A mouse anti-human CYR-61 monoclonal antibody was constructed using a conventional approach and screened by fluorescence-activated cell sorting (FACS). The full length of the anti-CYR-61 antibody was constructed, as previously described (24). The single chain variable fragments of the mouse anti-human CYR-61 monoclonal antibody (Sino Biological, Beijing, China) were cloned and inserted into a Pklight vector (termed Pklight-anti-CYR-61 vector; Biovector NTCC, Inc., Beijing, China). The constant domain heavy chain Fc and light chain fragments of mouse anti-human CYR-61 monoclonal antibody were subcloned into the Pklight-anti-CYR-61 vector. Pklight-anti-human CYR-61 monoclonal antibody and IREX-enhanced green fluorescent protein (EGFP) were subcloned into the Peedual12.4 vector (BioVector NTCC, Inc.), which contained the glutamine synthetase gene. The CHO-K1SV cell line (American Type Culture Collection) was cultured in Iscove's modified Dulbecco's medium (Sigma-Aldrich; Merck KGaA) supplemented with 10% fetal bovine serum and 2 mM L-glutamine. Peedual12.4-anti-human CYR-61 monoclonal antibody was transfected into the fluorescein isothiocyanate (Shanghai Xinyu Biotechnology Pharmaceutical Co., Ltd.)-labeled CHO-K1SV cells ($1x10^5$ cells/ml) using Lipofectamine 2000 (Tiangen Biotech Co., Ltd., Beijing, China). CHO-K1SV cells were washed and resuspended in 0.01 mol/l pH=7.4 PBS twice. The cells were identified and sorted in a flow cytometer at 488 nm. Thus, anti-human CYR-61 monoclonal antibody and EGFP were stably expressed in the CHO-K1SV cells. Stable and high expression of anti-CYR-61 antibodies in bacterial cells was screened using FACS (BD Biosciences, Franklin Lakes, NJ, USA). Data analysis and statistics were performed using BD Accuri™ C6 Plus (BD Biosciences) and GraphPad Prism 5 (GraphPad Software, Inc., La Jolla, CA, USA).

MTT assay. A total of 3,000 of H358 cells were cultured into each well of a 96-well plate and cells were used to investigate the inhibitory effects of anti-CYR-61 on cell viability when ~90% cell confluence was reached. Anti-CYR-61 (1:1,000) or 30 μl PBS (control) were added into each well of the 96-well plate and incubated at 37˚C for 12 h. Subsequently, 10 μl MTT (5 mg/ml; Sigma-Aldrich; Merck KGaA) was added to the cells and incubated at 37˚C for 4 h. Following this, dimethylsulfoxide (Amresco, LLC, Solon, OH, USA) was added for incubation for 30 min to dissolve the precipitate after the supernatant had been removed. Results were determined using a spectrophotometer (Bio-Rad Laboratories, Inc., Hercules, CA, USA) at 540 nm.

Reverse transcription-quantitative polymerase chain reaction (RT-qPCR). Total RNA was extracted from H358 cells and a normal lung cell line MRC-5 cells with or without treatment of anti-CYR-61 using an RNeasy mini kit (Qiagen Sciences, Inc., Gaithersburg, MD, USA), according to the manufacturer's protocol. RNA (1.0 μg) was reverse transcribed into cDNA using QuantiTect Reverse Transcription kit (Qiagen Sciences, Inc.), according to the manufacturer's protocol. The primers (Table I) were designed using Primer Express software (version 2.0; Thermo Fisher Scientific, Inc.) qPCR analysis was

performed using the SYBR® *Premix™ Ex Taq™* (Perfect Real Time; Takara Biotechnology Co., Ltd., Dalian, China) in a total volume of 20 μl using a 7300 Real-Time PCR System (Thermo Fisher Scientific, Inc.), according to the manufacturer's protocol. The thermocycling conditions were as follows: 95˚C for 30 sec, and 40 cycles of 95˚C for 5 sec and 60˚C for 30 sec. All relative mRNA expression levels were calculated using the by $2^{-\Delta\Delta Cq}$ method (25). Results were expressed as the n-fold relative to the housekeeping gene, β-actin.

ELISA. The affinity of anti-CYR-61 was examined for its target antigens, CYR-61, using ELISA in H358 cells. CYR-61 (0.2-1.4 mg/ml) was added into an enzyme-linked-immuno microplate and incubated at 4˚C for 12 h. Anti-CYR-61 (4 μg/ml) was added to the wells and incubated for 60 min at 37˚C, and bovine serum albumin (BSA; Atlanta Biologicals, Inc., Flowery Branch, GA, USA) was used as a control. Subsequently, 100 μl human horseradish peroxidase-conjugated CYR-61 antibodies (1:1,000; eBioscience, Inc.; Thermo Fisher Scientific, Inc.) was added and incubated at 37˚C for 60 min. The 3,3'-diaminobenzidine/H_2O_2 system was used for the detection of anti-CYR-61 affinity. Results were analyzed at 450 nm using an ELISA plate reader (Bio-Rad Laboratories, Inc.).

Cell invasion and migration assays. H358 cells were treated with anti-CYR-61 and non-treated H358 cells were used as control. H358 cells were adjusted to a density of $1x10^6$ cells in 500 μl serum-free RPMI-1640 medium for the invasion assay. H358 cells were treated with anti-CYR-61 (1:1,000) for 12 h at room temperature and then added to the tops of BD BioCoat Matrigel Invasion Chambers (BD Biosciences), according to the manufacturer's protocol. Transwell chambers (Costar; Corning Incorporated, Corning, NY, USA) with 8 μm diameter pores were utilized. Matrigel (100 μl; BD Biosciences, San Jose, CA, USA) was added to the Transwell apparatus. A total of 106 H358 cells in 100 μl serum-free culture medium (Gibco; Thermo Fisher Scientific, Inc.) was placed in the upper chamber and 500 μl complete culture medium containing 20% fetal bovine serum (Sigma-Aldrich; Merck KGaA) was added to the lower chamber as a chemoattractant. Following incubation at 37˚C for 24 h, Transwell chambers were stained with 0.4% crystal violet for 5 min at room temperature and washed with PBS three times. Non-migrating and non-invading cells were carefully wiped from the upper chambers with cotton wool. Results were examined using a CX21 Olympus light microscope (Olympus Corporation, Tokyo, Japan; magnification, x100).

For the migration assay, H358 ($1x10^4$) cells were inoculated with anti-CYR-61 (1:1,000) for 12 h at room temperature and Control inserts (BD Biosciences) were used instead of a Matrigel Invasion Chamber. Tumor cell invasion and migration were observed in at least three stained fields in every membrane using a light microscope at a magnification of x100. The invasion and migration assays used 24 well dishes.

Apoptosis assay. Apoptosis was determined by staining H358 cells with Annexin V-PE/ and 7-aminoactinomycin (BD Biosciences) for 15 min at 25˚C in the dark, and flow cytometry analysis was performed. The Annexin V-positive cells were counted as early apoptotic cells. 7-amino actinomycin-positive cells were counted as necrotic cells. Double positive cells were counted as late apoptotic cells. Double negative cells were counted as live cells.

Animal study. A total of 50 female specific pathogen-free C57BL/6 mice (aged 6-8 weeks; weighing 20±2 g) were purchased from Shanghai Slack Experimental Animals Co., Ltd., (Shanghai, China). The mice were given free accessible to food and water, and were housed at 20˚C with 60% humidity and 12 h light/dark cycle. C57BL/6 mice were subcutaneously implanted with H358 tumor cells and were divided into two groups (20 per group). Treatments were initiated on day 5 after tumor implantation when the tumor diameter had reached 6-8 mm. H358-bearing mice were intravenously injected with anti-CYR-61 or 10 μl PBS as a control. The treatment was administered once daily for 14 days. Tumor volumes were calculated according to previous study (26). The survival rate for animals treated with anti-CYR-61 (1:1,000) or 10 μl PBS was detected during a 120-day observation period.

Western blotting. Total protein was extracted using CytoBuster™ Protein Extraction Reagent (EMD Millipore, Billerica, MA, USA) and protein concentration was measured by the *DC™* Protein Assay (Bio-Rad Laboratories, Inc.) using the Bradford method (27). A total of 40 μg of protein from each sample were separated by 10% SDS-PAGE and transferred to an equilibrated polyvinylidene difluoride membrane (GE Healthcare, Chicago, IL, USA). The membrane was blocked by 5% milk in 0.1% Tween 20 in Tris-buffer solution (TBS) at room temperature for 1 h. After incubation with specific primary antibody at 4˚C overnight and the membranes were washed four times with TBS, 10 min each time. The membranes were then incubated with horseradish peroxidase-conjugated secondary antibodies (1:800; cat. no. ab7090; Abcam, Cambridge, MA, USA) at 37˚C for 30 min and the proteins were detected by enhanced chemiluminescence (GE Healthcare) and quantified using an image analyzer Quantity One System (Bio-Rad Laboratories, Inc.). The primary antibodies directed against CYR-61 (cat. no. ab24448), extracellular signal-regulated kinase (cat. no. ab54230), AKT (cat. no. ab8805), phosphorylated (p)ERK (cat. no. ab79483), pAKT (cat. no. ab8933), fibronectin (cat. no. ab23750), SMA (cat. no. ab21027) and N-cadherin (cat. no. ab98952) were purchased from Abcam (Cambridge, UK) all at a dilution of 1:500 and were incubated at 4˚C overnight. Primary antibodies directed against Caspase 8 (1;800; cat. no, sc81656), 9 (1;800; cat. no. sc56076) and 10 (1;800; cat. no. sc134299), Fas ligand (FasL; 1;800; cat. no. sc33716), Fas-associated protein with Death Domain (FADD; 1:800; cat. no. sc5559), apoptotic protease activating factor 1 (Apaf-1; 1:800; cat. no. sc135836), B cell lymphoma-2 antagonist/killer (Bak; 1:800; cat. no. sc517390), B cell lymphoma-2-associated X protein (Bax; 1:800; cat. no. sc20067), vimentin (1:800; cat. no. sc80975) were purchased from Santa Cruz Biotechnology, Inc. (Dallas, TX, USA). The housekeeping proteins β-actin (1:500; cat. no. 3700) and GAPDH (1:500; cat. no. 97166) were purchased from Cell Signaling Technology, Inc. (Danvers, MA, USA). Density analysis was performed using Image J v.1.49 (National Institutes of Health, Bethesda, MD, USA).

Histological immunostaining. For immunostaining, H358 cells or tumors from xenograft mice with NSCLC were fixed using

Table I. Primer sequences utilized in RT-qPCR.

Gene	Primer	Sequence
CYR-61	Forward	5'-CAAGGAGCTGGGATTCGATG-3'
	Reverse	5'-AAAGGGTTGTATAGGATGCGAG-3'
Bak	Forward	5'-CACCTTACCTCTGCAACCTAG-3'
	Reverse	5'-TGCAACATGGTCTGGAACTC-3'
Bax	Forward	5'-AGTAACATGGAGCTGCAGAG-3'
	Reverse	5'-AGTAGAAAAGGGCGACAACC-3'
Caspase-9	Forward	5'-GTTTGAGGACCTTCGACCAG-3'
	Reverse	5'-GCATTAGCGACCCTAAGCAG-3'
Apaf-1	Forward	5'-CCTCTCATTTGCTGATGTCG-3'
	Reverse	5'-TCACTGCAGATTTTCACCAGA-3'
Caspase-10	Forward	5'-AATCTGACATGCCTGGAG-3'
	Reverse	5'-ACTCGGCTTCCTTGTCTAC-3'
Caspase-8	Forward	5'-ATGCAAACTGGATGATGACA-3'
	Reverse	5'-TTCATATCTTCAGCAGGTCT-3'
FasL	Forward	5'-AACCAAGTGGACCTTGAGACCACA-3'
	Reverse	5'-TTCACATGGCAGCCCAGAGTTCTA-3'
FADD	Forward	5'-CCTGGTACAAGAGGTTCAGC-3'
	Reverse	5'-CTGTGTAGATGCCTGTGGTC-3'
β-actin	Forward	5'-ACCTTCTACAATGAGCTGCG-3'
	Reverse	5'-CCTGGATAGCAACGTACATGG-3'

10% formaldehyde at room temperature for 24 h and subsequently embedded in paraffin. Following this, tumor samples were sliced into 4-μm-thick sections and antigen retrieval was also performed with 0.1 M citrate buffer for 15 min at 100˚C, rehydrated in a descending series of ethanol (100, 95, 85, 80 and 75%) watched in xylene in tumor sections. After blocking by 10% BSA at room temperature for 1 h, H358 cells and tumor sections were incubated with pERK (cat. no. ab192591), pAKT (cat. no. ab38449) and CYR-61 (cat. no. ab24448; all 1:600; Abcam) primary antibodies at 37˚C for 2 h. Following washing three times with TBST, HRP-conjugated goat anti-rabbit Immunoglobulin G secondary antibodies (1:800; cat. no. ab97051; Abcam) were incubated 30 min at 37˚C. Specimens were then visualized using a binocular light microscope (Eclipse E100-LED; Nikon Corporation, Tokyo, Japan) at a magnification of x200. A Ventana Benchmark automated staining system (Ventana Medical Systems, Inc., Tucson, AZ, USA) was used for observation of CYR-61.

Statistical analysis. All data were presented as the mean ± standard deviation of triplicates. Unpaired data were compared using Student's t-tests and comparisons of data between multiple groups were made using one-way analysis of variance with a post-hoc Tukey's test using SPSS 17.0 software (SPSS, Inc., Chicago, IL, USA). Kaplan-Meier tests were used to estimate the survival rate during 120-day long-term treatment. $P<0.05$ was considered to indicate a statistically significant difference.

Results

CYR-61 expression and anti-CYR-61 characteristics. In order to analyze the role of CYR-61 in NSCLC, mRNA and protein expression levels of CYR-61 were detected in the NSCLC cell line H358 and a normal lung cell line MRC-5 by RT-qPCR analysis and western blotting. The results demonstrated that CYR-61 mRNA expression levels were significantly higher ($P<0.01$) and protein expression levels were markedly higher in the H358 cell line compared with the levels in the MRC-5 cell line (Fig. 1A). These findings suggested that CYR-61 was a potential molecular target for NSCLC. Therefore, a full-length antibody was constructed to target CYR-61, termed anti-CYR-61, which was screened by flow cytometry. The population of CYR-61 positive cells began to reduce 1 h after anti-CYR-61 treatment, and reduced to its lowest level 3 h after the treatment (Fig. 1B). An ELISA assay of anti-CYR-61 demonstrated a high affinity with CYR-61 (Fig. 1C). Western blotting revealed that anti-CYR-61 was 76 kDa under non-reducing conditions (Fig. 1D). Western blotting also demonstrated that anti-CYR-61 was able to specifically bind with CYR-61. These results indicated that CYR-61 was upregulated in NSCLC cell lines and that the anti-CYR-61 antibodies we constructed exhibited high affinity for CYR-61.

Effect of anti-CYR-61 on CYR-61-induced NSCLC viability, migration and invasion. To identify the function of CYR-61 in NSCLC, we investigated the inhibitory effects of anti-CYR-61 on cell viability, migration and invasion of H358 cells. As demonstrated in Fig. 2A and B, H358 cell viability was significantly inhibited following treatment with anti-CYR-61, which decreased CYR-61 expression ($P<0.01$). In migration and invasion assays, anti-CYR-61 treatment inhibited the migration and invasion of H358 cells (Fig. 2C and D). These results indicated that anti-CYR-61 may have potential therapeutic effects by inhibiting NSCLC cell viability, migration and invasion by targeting CYR-61.

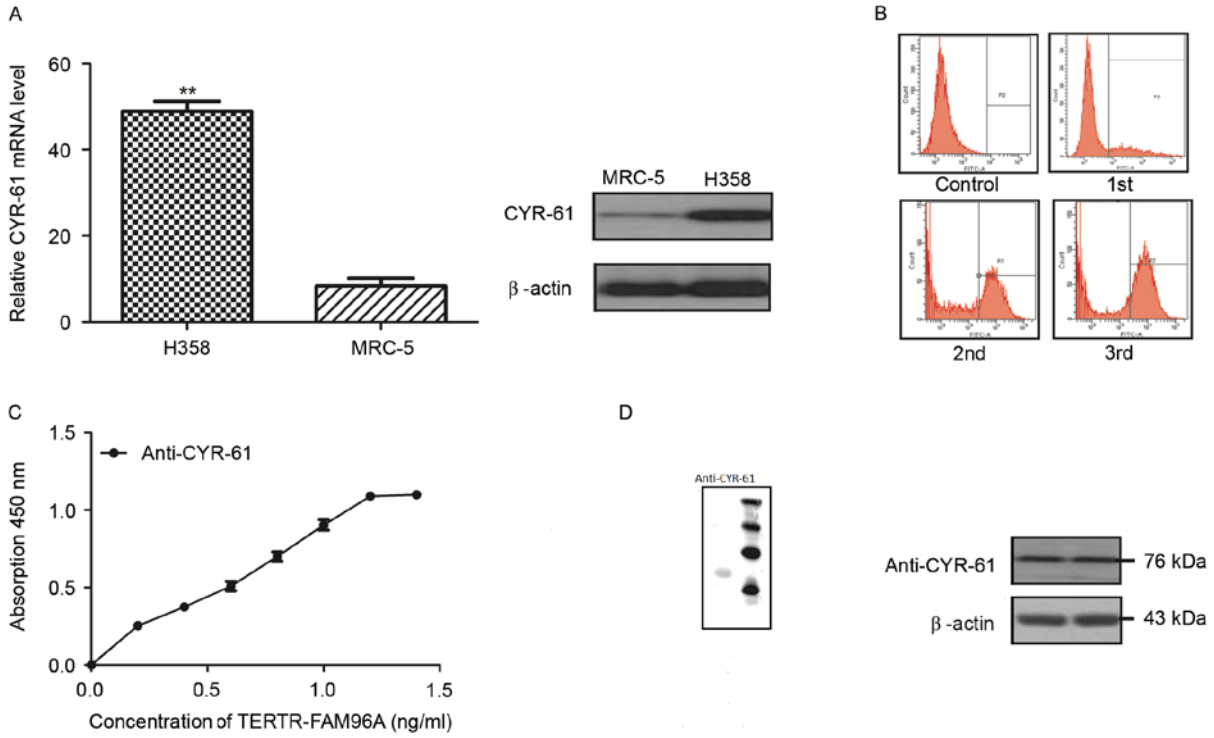

Figure 1. Expression of CYR-61 in NSCLC and normal lung cell line and the characteristics of anti-CYR-61. (A) Reverse transcription-quantitative polymerase chain reaction and western blot analyses were used to analyze the expression of CYR-61 in H358 NSCLC cells and MRC-5 normal lung cells. Data are presented as the mean ± SD of triplicate samples. (B) Fluorescence-activated cell sorting was used to screen anti-CYR-61affinity. 1st, 2nd and 3rd represent the population of CYR-61 positive cells 1, 2 and 3 h after anti-CYR-61 treatment, respectively. (C) ELISA was used to analyze the affinity of anti-CYR-61 for its target protein, CYR-61. Data are presented as the mean ± SD of triplicate samples. (D) Western blotting was used to analyze the purified anti-CYR-61. **P<0.01 vs. MRC-5 cells. CYR-61, cysteine-rich angiogenic inducer-61; SD, standard deviation; TERTR-FAM96A, telomerase reverse transcriptase-family with sequence similarity 96 member A; NSCLC, non-small cell lung cancer.

Effect of anti-CYR-61 on NSCLC cell migration and the AKT and ERK signaling pathways. To further investigate the effects and mechanism of anti-CYR-61 on cell migration, we analyzed ERK and AKT expression and phosphorylation levels in H358 cells prior to and following treatment with anti-CYR-61. As demonstrated in Fig. 3A and B, anti-CYR-61 treatment significantly suppressed AKT and ERK protein expression and phosphorylation compared with untreated controls (P<0.01), indicating a reduction in AKT and ERK activity in NSCLC cells treated with anti-CYR-61. Immunofluorescence also indicated that expression and phosphorylation levels of AKT and ERK were inhibited in H358 cells treated with anti-CYR-61 (Fig. 3C and D). These results suggested that the inhibitory effect of anti-CYR-61 on migration may involve AKT and ERK phosphorylation and the ERK and AKT signaling pathways.

Role of anti-CYR-61 on cell apoptosis. As the results demonstrated that anti-CYR-61 regulated NSCLC cell migration through phosphorylation of ERK and AKT process, the apoptotic effects of anti-CYR-61 on H358 cells by blocking the CYR-61 were analyzed. NSCLC H358 cells were treated with or without anti-CYR-61. Results demonstrated that anti-CYR-61 significantly promoted H358 cell apoptosis compared with the control cells (P<0.01; Fig. 4A). In addition, the relationship between anti-CYR-61 and apoptosis signaling pathways in H358 cells was investigated. Results indicated that FasL, FADD, caspase-8 and -10 mRNA expression levels were significantly elevated by anti-CYR-61 treatment compared with the control cells (P<0.01; Fig. 4B). Western blot analysis also revealed that FasL, FADD, caspase-8 and -10 protein expression levels were markedly upregulated following treatment with anti-CYR-61 compared with control cells (Fig. 4C). However, no significant difference in the expression levels of Bak, Bax, Apaf-1 and caspase-9 were observed between anti-CYR-61-treated cells and the control cells (Fig. 4D and E). These results suggested that anti-CYR-61 has an important role in regulating exogenous cell apoptosis signaling pathways for NSCLC cells.

Anti-tumor effects of anti-CYR-61 in mice with NSCLC. Following observation of the inhibitory effects of anti-CYR-61 on NSCLC cell viability *in vitro*, the anti-tumor efficacy of anti-CYR-61 in H358-bearing mice was investigated *in vivo*. As illustrated in Fig. 5A, tumor growth was significantly inhibited 21 days after anti-CYR-61 treatment, as determined via tumor volume, compared with PBS-treated mice (P<0.01). In addition, immunohistology demonstrated that CYR-61 expression was downregulated in anti-CYR-61-treated tumors compared with PBS-treated tumors (Fig. 5B). In agreement with the *in vitro* results, the findings demonstrated that AKT and ERK expression were decreased in tumors from experimental mice treated with anti-CYR-61 on day 25 compared with control mice treated with PBS (Fig. 5C). To analyze the relationship between anti-CYR-61 and the EMT process *in vivo*, EMT biomarker expression levels of vimentin, fibronectin, SMA and N-cadherin were analyzed. The results in Fig. 5D demonstrated that the protein expression levels of EMT markers were decreased

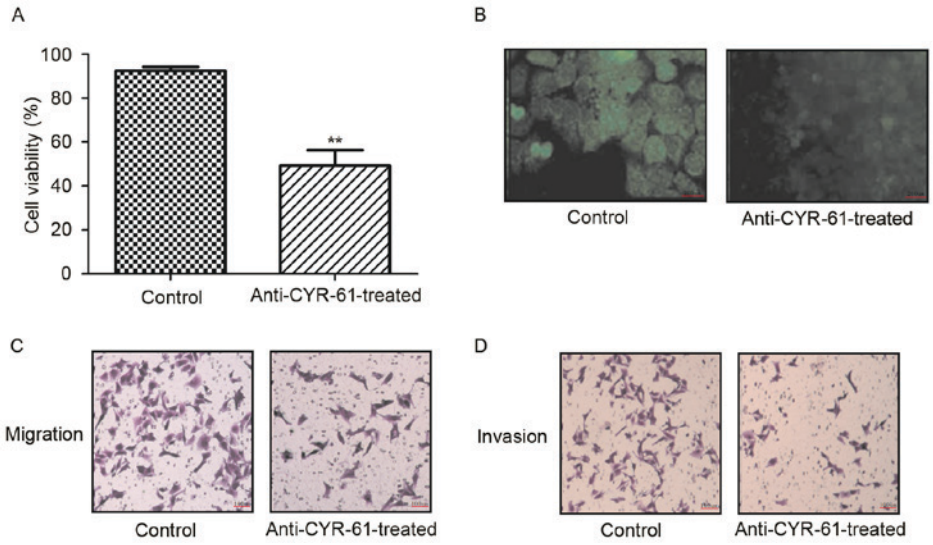

Figure 2. Inhibitory effects of anti-CYR-61 on H358 cells *in vitro*. (A) MTT assays were used to analyze the inhibitory effects of anti-CYR-61 on H358 cell viability. (B) Immunofluorescence (using Alexa Fluro® conjugated Goat anti-rabbit Immunoglobulin G) was used to detect CYR-61 expression after anti-CYR-61 treatment. (C) Migration analysis was performed to determine the effect of anti-CYR-61 on H358 cell migration. (D) Invasion analysis was performed to determine the effect of anti-CYR-61 on H358 cell invasion. C and D were stained using hematoxylin and eosin. Data was presented as the mean ± standard deviation of triplicate samples. **P<0.01 vs. the control. CYR-61, cysteine-rich angiogenic inducer-61.

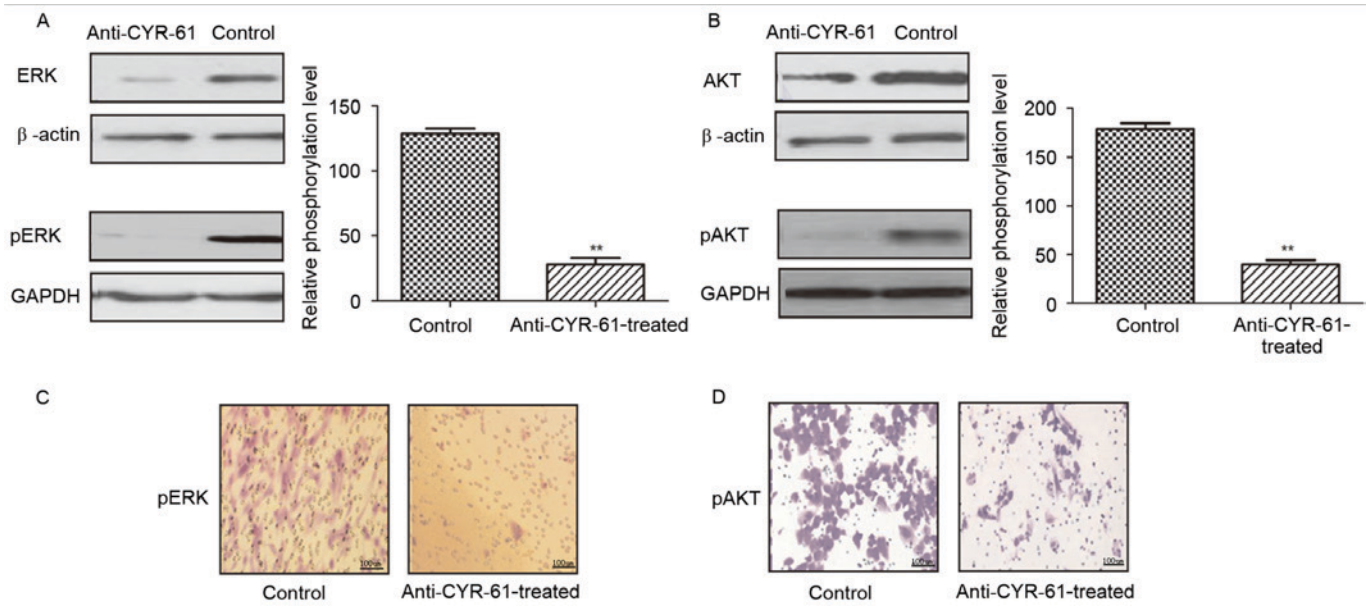

Figure 3. Downregulation of ERK and AKT phosphorylation induced by anti-CYR-61. (A) Expression levels of ERK were analyzed using western blotting after treatment with anti-CYR-61. (B) Expression levels of AKT were analyzed by western blotting after treatment with anti-CYR-61. (C) Phosphorylation levels of ERK were analyzed in tumor sections following treatment with anti-CYR-61. Red arrows demonstrate positive pERK expression. (D) Phosphorylation levels of AKT were analyzed in tumor sections after treatment with anti-CYR-61. Red arrows demonstrate positive pAKT expression. Data are presented as the mean ± standard deviation of triplicate samples. **P<0.01 vs. the Control. ERK, extracellular signal-regulated kinase; AKT, protein kinase B; CYR-61, cysteine-rich angiogenic inducer-61; p, phosphorylated.

in anti-CYR-61-treated tumors compared with PBS-treated tumors. Furthermore, it was observed that the survival rate of Anti-CYR-61 treatment is significantly higher than that of PBS treatment after day 40 during a 120-day observation period (P<0.01; Fig. 5E). Anti-CYR-61 treatment significantly inhibited tumor metastasis compared with PBS-treated mice (P<0.01; Fig. 5E and F). In conclusion, our findings suggested that anti-CYR-61 presented potential anti-cancer efficacy in NSCLC treatment in murine model.

Discussion

The incidence and mortality rate of human lung cancer has been growing rapidly in recent years and is one of the most threatening types of malignant tumors to health and survival (28). NSCLC represents more than 85% of lung cancer cases according to statistical clinical data (29). Therefore, NSCLC has attracted much attention to identify anti-cancer agents, ranging from molecular markers to immunotherapy, in order to improve

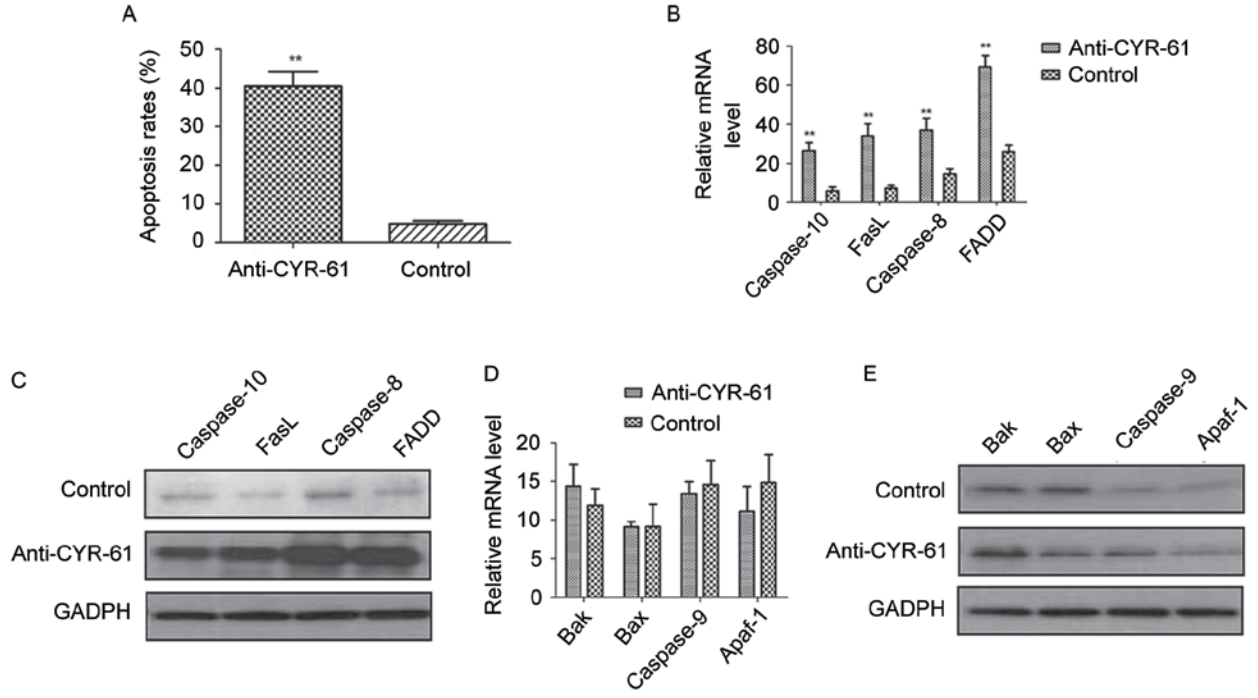

Figure 4. Effect of anti-CYR-61 on apoptosis in NSCLC cells. (A) Fluorescence-activated cell sorting was used to evaluate the apoptosis of H358 cells after anti-CYR-61 treatment. Apoptosis-related (B) mRNA and (C) protein expression levels in an exogenous cell apoptosis signaling pathway were analyzed in anti-CYR-61-treated cells. Apoptosis-related (D) mRNA and (E) protein expression levels in the mitochondrial apoptosis pathway were analyzed in anti-CYR-61-treated cells. Data are presented as the mean ± standard deviation of triplicate samples. **P<0.01 vs. the control. CYR-61, cysteine-rich angiogenic inducer-61; NSCLC, non-small-cell lung cancer; FasL, Fas ligand; FADD, Fas-associated protein with Death Domain; Bak, B cell lymphoma-2 antagonist/killer; Bax, B cell lymphoma-2-associated X protein; Apaf-1, apoptotic protease activating factor 1.

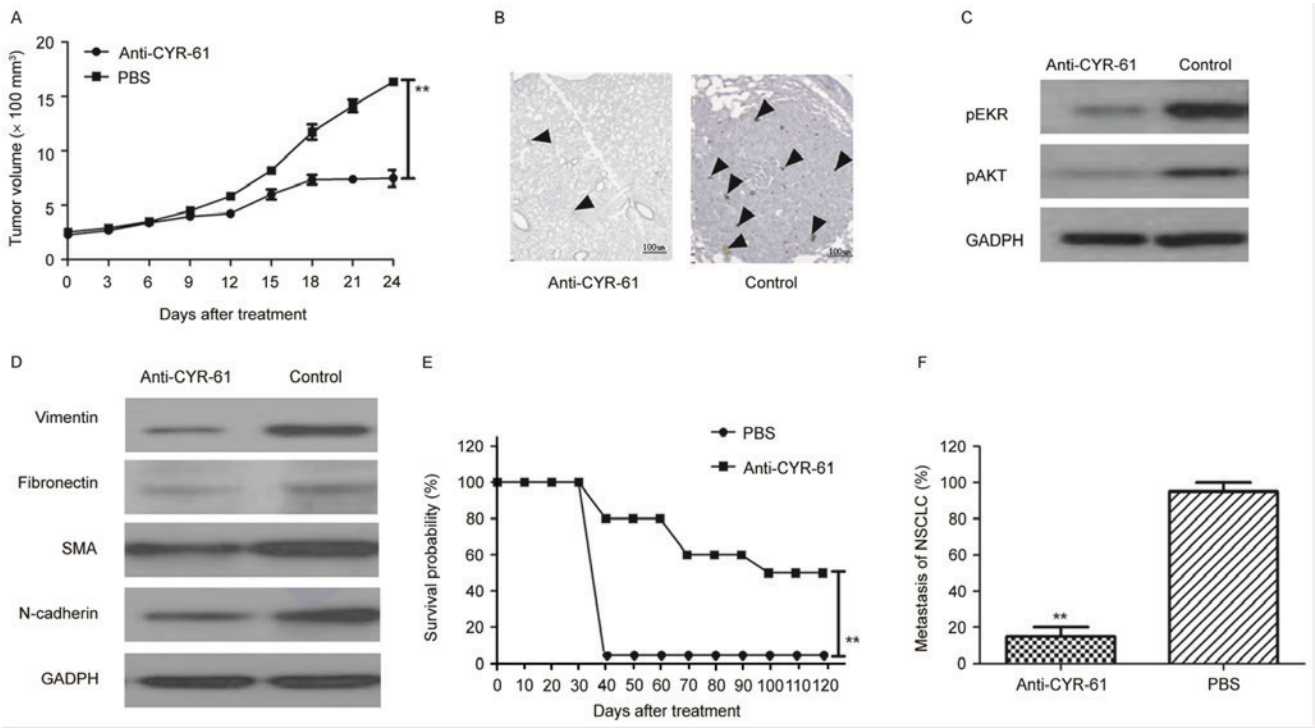

Figure 5. Therapeutic and metastasis effects of anti-CYR-61 in H358-bearing mice. (A) Tumor growth was analyzed during a 24-day short-term observation period. Data are presented as the mean ± SD. **P<0.01 vs. PBS on day 21. (B) CYR-61 expression was analyzed after anti-CYR-61 treatment and DAB staining. Black arrows, *in situ* CYR-61 (C) Phosphorylation levels of ERK and AKT were analyzed by western blotting in tumors following treatment with anti-CYR-61. (D) EMT biomarker expression levels were analyzed by western blotting in tumors following treatment with anti-CYR-61. (E) Long-term survival probability was compared over a 120-day observation between the anti-CYR-61 and PBS treatment groups. It was demonstrated that the survival rate of Anti-CYR-61 treatment was significantly higher than that of PBS treatment after day 40 during the 120 day observation period. (F) NSCLC metastasis was analyzed in experimental mice. Data are expressed as the mean ± SD. **P<0.01 vs. PBS. CYR-61, cysteine-rich angiogenic inducer-61; ERK, extracellular signal-regulated kinase; AKT, protein kinase B; EMT, epithelial-mesenchymal transition; PBS, phosphate-buffered saline; NSCLC, non-small cell lung cancer; p, phosphorylated; SMA, α-smooth muscle actin; SD, standard deviation.

the treatment and prognosis of patients with NSCLC. Notably, the majority of newly diagnosed NSCLC cases are often in the moderate or severe stage, decreasing the recovery probability and survival period (30). Therapeutic protocols for advanced NSCLC have expanded to include a number of targeted interventions, including chemotherapy, radiotherapy, small molecule target therapy, personalized treatment and immunotherapy (31). Various types of treatment for NSCLC have been introduced with different mechanisms of action; they have been shown to change tumor architecture and the tumor microenvironment, however the outcomes were not promising as an early reduction in tumor mass was not achieved (32). The reasons of treatment failure were predominantly that these treatments failed to control NSCLC migration and inhibit invasion in patients during treatment periods.

CYR-61 is a secreted protein of the CCN family that is associated with the extracellular matrix signaling pathway. Previous research has indicated that CYR-61 is potent in regulating tumor cell activities, such as tumor cell growth, apoptosis, proliferation, migration, adhesion, differentiation and the EMT process, in the majority of human cancer cells (17). A study by Sabile *et al* (33) reported that CYR-61 signaling was regulated by phosphorylation of AKT and ERK in osteosarcoma tumor and lung cancer cells. In addition, a study by Chen *et al* (34) described that phosphorylation of AKT and ERK was significantly associated with the migration and invasion of prostate carcinoma PC-3 cells. In the present study, a full-length antibody target for CYR-61 was constructed and its anti-tumor efficacy in a murine model of lung cancer was investigated. In agreement with results from a previous report (35), the present study demonstrated that anti-CYR-61 treatment inhibited phosphorylation of the AKT and ERK signaling pathway in human NSCLC cells. Furthermore, it was demonstrated that anti-CYR-61 inhibited tumor growth and downregulated EMT biomarker expression of vimentin, fibronectin, SMA and N-cadherin.

In a previous report, CYR-61 expression was demonstrated to be downregulated via inhibition of the ERK and AKT pathways, resulting in suppression of colon cancer cell migration (19). A study by Lee *et al* (36) suggested that activities of CYR-61 protein were modulated through extracellular acidification and the PI3K/AKT signaling pathway in prostate carcinoma cells. Furthermore, Chen *et al* (34) indicated that transforming growth factor-β induced CYR-61 production to enhance tumor cell migration and invasion *in vitro* and *in vivo*. These observations were supported in the present study in NSCLC cells and the results of the present study also suggested that inhibition of CYR-61 production is beneficial for inhibiting NSCLC cell viability, migration and invasion via the AKT and ERK signaling pathways.

In the present study, CYR-61 production in human NSCLC cells and normal lung cells was investigated. The critical role of the CYR-61 signaling pathway for the EMT process was confirmed in NSCLC H358 cells. Previous research has reported that activation of ERK and the PI3K/AKT signal pathway has an important role in regulation of tumor cell migration (37). In the present study, antibody targeting of CYR-61 not only inhibited viability of NSCLC H358 cells, it also suppressed migration of NSCLC H358 cells *in vitro* and *in vivo*.

In conclusion, the aim of the present study was to investigate the association between CYR-61 and the prognosis of NSCLC in a murine model. Anti-CYR-61was demonstrated to be a potential anti-tumor agent for NSCLC by targeting CYR-61, which led to inhibition of migration by decreasing the production of CYR-61 via suppressing phosphorylation of AKT and ERK. Taken together, the therapeutic efficacy of anti-CYR-61 was examined and the results suggested that this targeted strategy may represent an attractive method of inhibiting tumor cell migration for the treatment of NSCLC.

Acknowledgements

Not applicable.

Funding

No funding was received.

Availability of data and materials

The datasets used and/or analyzed during the current study are available from the corresponding author on reasonable request.

Authors' contributions

XL and YQ constructed and performed the cell invasion and migration assays, and were major contributors in writing the manuscript. NY analyzed and interpreted the RT-qPCR, western blotting and histological immunostaining data. LL performed and analyzed the animal study and ELISA assay. LY performed and analyzed the MTT and apoptosis assays.

Ethics approval and consent to participate

The present study was carried out in strict accordance with the approval and recommendations from the Ethics Committee of the Care and Use of Laboratory Animals of Qilu Hospital of Shandong University (Jinan, China). All surgery and euthanasia were performed under sodium pentobarbital anesthesia, and all efforts were made to minimize suffering.

Consent for publication

Not applicable.

Competing interests

The authors declare that they have no competing interests.

References

1. Fenton-Ambrose L and Kazerooni EA: Preventative care: Lung-cancer screens now worth the cost. Nature 514: 35, 2014.
2. Awad R and Nott L: Radiation recall pneumonitis induced by erlotinib after palliative thoracic radiotherapy for lung cancer: Case report and literature review. Asia Pac J Clin Oncol 12: 91-95, 2016.
3. Jiang SY, Zhao J, Wang MZ, Huo Z, Zhang J, Zhong W and Xu Y: Small-cell lung cancer transformation in patients with pulmonary adenocarcinoma: A case report and review of literature. Medicine (Baltimore) 95: e2752, 2016.

4. Kong R, Feng J, Ma Y, Zhou B, Li S, Zhang W, Jiang J, Zhang J, Qiao Z, Zhang T, *et al*: Silencing NACK by siRNA inhibits tumorigenesis in non-small cell lung cancer via targeting Notch1 signaling pathway. Oncol Rep 35: 2306-2314, 2016.
5. Brody H: Lung cancer. Nature 513: S1, 2014.
6. Moro-Sibilot D, Smit E, de Castro Carpeño J, Lesniewski-Kmak K, Aerts JG, Villatoro R, Kraaij K, Nacerddine K, Dyachkova Y, Smith KT, *et al*: Non-small cell lung cancer patients with brain metastases treated with first-line platinum-doublet chemotherapy: Analysis from the European FRAME study. Lung Cancer 90: 427-432, 2015.
7. Barnett SA, Downey RJ, Zheng J, Plourde G, Shen R, Chaft J, Akhurst T, Park BJ and Rusch VW: Utility of routine PET imaging to predict response and survival after induction therapy for non-small cell lung cancer. Ann Thorac Surg 101: 1052-1059, 2016.
8. Xie FJ, Lu HY, Zheng QQ, Qin J, Gao Y, Zhang YP, Hu X and Mao W: The clinical pathological characteristics and prognosis of FGFR1 gene amplification in non-small-cell lung cancer: A meta-analysis. Onco Targets Ther 9: 171-181, 2016.
9. Lim SH, Sun JM, Lee SH, Ahn JS, Park K and Ahn MJ: Pembrolizumab for the treatment of non-small cell lung cancer. Expert Opin Biol Ther 16: 397-406, 2016.
10. Müller B, Bovet M, Yin Y, Stichel D, Malz M, González-Vallinas M, Middleton A, Ehemann V, Schmitt J, Muley T, *et al*: Concomitant expression of far upstream element (FUSE) binding protein (FBP) interacting repressor (FIR) and its splice variants induce migration and invasion of non-small cell lung cancer (NSCLC) cells. J Pathol 237: 390-401, 2015.
11. Zhao Q, Yue J, Zhang C, Gu X, Chen H and Xu L: Inactivation of M2 AChR/NF-κB signaling axis reverses epithelial-mesenchymal transition (EMT) and suppresses migration and invasion in non-small cell lung cancer (NSCLC). Oncotarget 6: 29335-29461, 2015.
12. Zhang H, Zhu X, Li N, Li D, Sha Z, Zheng X and Wang H: miR-125a-3p targets MTA1 to suppress NSCLC cell proliferation, migration, and invasion. Acta Biochim Biophys Sin (Shanghai) 47: 496-503, 2015.
13. Roth MT, Ivey JL, Esserman DA, Crisp G, Kurz J and Weinberger M: Individualized medication assessment and planning: Optimizing medication use in older adults in the primary care setting. Pharmacotherapy 33: 787-797, 2013.
14. Lin Y, Xu T, Tian G and Cui M: Cysteine-rich, angiogenic inducer, 61 expression in patients with ovarian epithelial carcinoma. J Int Med Res 42: 300-306, 2014.
15. Xu ST, Ding X, Ni QF and Jin SJ: Targeting MACC1 by RNA interference inhibits proliferation and invasion of bladder urothelial carcinoma in T24 cells. Int J Clin Exp Pathol 8: 7937-7944, 2015.
16. Han S, Bui NT, Ho MT, Kim YM, Cho M and Shin DB: Dexamethasone inhibits TGF-β1-induced cell migration by regulating the ERK and AKT pathways in human colon cancer cells via CYR61. Cancer Res Treat 48: 1141-1153, 2016.
17. Osaki M, Inaba A, Nishikawa K, Sugimoto Y, Shomori K, Inoue T, Oshimura M and Ito H: Cysteine-rich protein 61 suppresses cell invasion via down-regulation of matrix metalloproteinase-7 expression in the human gastric carcinoma cell line MKN-45. Mol Med Rep 3: 711-715, 2010.
18. Hviid CV, Erdem JS, Kunke D, Ahmed SM, Kjeldsen SF, Wang YY, Attramadal H and Aasen AO: The matri-cellular proteins 'cysteine-rich, angiogenic-inducer, 61' and 'connective tissue growth factor' are regulated in experimentally-induced sepsis with multiple organ dysfunction. Innate Immun 18: 717-726, 2012.
19. Ito T, Hiraoka S, Kuroda Y, Ishii S, Umino A, Kashiwa A, Yamamoto N, Kurumaji A and Nishikawa T: Effects of schizophrenomimetics on the expression of the CCN1 (CYR 61) gene encoding a matricellular protein in the infant and adult neocortex of the mouse and rat. Int J Neuropsychopharmacol 10: 717-725, 2007.
20. Sabile AA, Arlt MJ, Muff R, Bode B, Langsam B, Bertz J, Jentzsch T, Puskas GJ, Born W and Fuchs B: Cyr61 expression in osteosarcoma indicates poor prognosis and promotes intratibial growth and lung metastasis in mice. J Bone Miner Res 27: 58-67, 2012.
21. Aoki M and Fujishita T: Oncogenic roles of the PI3K/AKT/mTOR axis. Curr Top Microbiol Immunol 407: 153-189, 2017.
22. Chen X, Cheng H, Pan T, Liu Y, Su Y, Ren C, Huang D, Zha X and Liang C: mTOR regulate EMT through RhoA and Rac1 pathway in prostate cancer. Mol Carcinog 54: 1086-1095, 2015.
23. Risolino M, Mandia N, Iavarone F, Dardaei L, Longobardi E, Fernandez S, Talotta F, Bianchi F, Pisati F, Spaggiari L, *et al*: Transcription factor PREP1 induces EMT and metastasis by controlling the TGF-β-SMAD3 pathway in non-small cell lung adenocarcinoma. Proc Natl Acad Sci USA 111: E3775-E3784, 2014.
24. Bai F, Tian H, Niu Z, Liu M, Ren G, Yu Y, Sun T, Li S and Li D: Chimeric anti-IL-17 full-length monoclonal antibody is a novel potential candidate for the treatment of rheumatoid arthritis. Int J Mol Med 33: 711-721, 2014.
25. Livak KJ and Schmittgen TD: Analysis of relative gene expression data using real-time quantitative PCR and the 2(-Delta Delta C(T)) method. Methods 25: 402-408, 2001.
26. Zhuang T, Djemil T, Qi P, Magnelli A, Stephans K, Videtic G and Xia P: Dose calculation differences between Monte Carlo and pencil beam depend on the tumor locations and volumes for lung stereotactic body radiation therapy. J Appl Clin Med Phys 14: 4011, 2013.
27. Lu TS, Yiao SY, Lim K, Jensen RV and Hsiao LL: Interpretation of biological and mechanical variations between the Lowry versus Bradford method for protein quantification. N Am J Med Sci 2: 325-328, 2010.
28. Jang BI and Hwang MJ: Do esophageal squamous cell carcinoma patients have an increased risk of coexisting colorectal neoplasms? Gut Liver 10: 6-7, 2016.
29. Kulkarni S, Vella ET, Coakley N, Cheng S, Gregg R, Ung YC and Ellis PM: The use of systemic treatment in the maintenance of patients with non-small cell lung cancer: A systematic review. J Thorac Oncol 11: 989-1002, 2016.
30. Yoshiba S, Jansen M, Matsushima N, Chen S and Mendell J: Population pharmacokinetic analysis of patritumab, a HER3 inhibitor, in subjects with advanced non-small cell lung cancer (NSCLC) or solid tumors. Cancer Chemother Pharmacol 77: 987-996, 2016.
31. Weller A, O'Brien MER, Ahmed M, Popat S, Bhosle J, McDonald F, Yap TA, Du Y, Vlahos I and deSouza NM: Mechanism and non-mechanism based imaging biomarkers for assessing biological response to treatment in non-small cell lung cancer. Eur J Cancer 59: 65-78, 2016.
32. Rossi A and Di Maio M: Platinum-based chemotherapy in advanced non-small-cell lung cancer: Optimal number of treatment cycles. Expert Rev Anticancer Ther 16: 653-660, 2016.
33. Sabile AA, Arlt MJ, Muff R, Husmann K, Hess D, Bertz J, Langsam B, Aemisegger C, Ziegler U, Born W and Fuchs B: Caprin-1, a novel Cyr61-interacting protein, promotes osteosarcoma tumor growth and lung metastasis in mice. Biochim Biophys Acta 1832: 1173-1182, 2013.
34. Chen J, Song Y, Yang J, Gong L, Zhao P, Zhang Y and Su H: The up-regulation of cysteine-rich protein 61 induced by transforming growth factor beta enhances osteosarcoma cell migration. Mol Cell Biochem 384: 269-277, 2013.
35. Wong WR, Chen YY, Yang SM, Chen YL and Horng JT: Phosphorylation of PI3K/Akt and MAPK/ERK in an early entry step of enterovirus 71. Life Sci 78: 82-90, 2005.
36. Lee YJ, Lee DM and Lee SH: Production of Cyr61 protein is modulated by extracellular acidification and PI3K/Akt signaling in prostate carcinoma PC-3 cells. Food Chem Toxicol 58: 169-176, 2013.
37. Shelton JG, Steelman LS, Lee JT, Knapp SL, Blalock WL, Moye PW, Franklin RA, Pohnert SC, Mirza AM, McMahon M and McCubrey JA: Effects of the RAF/MEK/ERK and PI3K/AKT signal transduction pathways on the abrogation of cytokine-dependence and prevention of apoptosis in hematopoietic cells. Oncogene 22: 2478-2492, 2003.